

Microfluidic systems for *in situ* formation of nylon 6,6 membranes

J. Gargiuli ^{a,*}, E. Shapiro ^b, H. Gulhane ^a, G. Nair ^a, D. Drikakis ^b, P. Vadgama ^a

^a*IRC in Biomedical Materials, Queen Mary, University of London, Mile End Road,*

E1 4NS, London, UK

^b*Fluid Mechanics and Computational Science Group, School of Engineering, Cranfield University,*

Cranfield, Bedfordshire, MK43 0AL, UK

Abstract

A microfluidics based, localised formation of nylon 6,6 membranes has been undertaken. The study demonstrates the feasibility of maintaining stable aqueous/organic interfaces for xylene within simple linear flow channels. Glass fabricated structures were used with adipoyl chloride and hexamethylenediamine in the organic and aqueous phases respectively, in order to achieve nylon 6,6 interfacial polymerisation. Localised membrane formation was investigated in flow channels of different geometries over a wide range of flow rates (500 to 4000 $\mu\text{l}/\text{min}$), with Reynolds numbers ranging from 8.4 to 67.2. The results demonstrate that interfacial polymerisation occurs consistently over a wide range of flow rates and of flow entry angles for dual aqueous/organic solvent input. However, creation of uniform planar film structures required careful optimisation, and these were best achieved at 2000 $\mu\text{l}/\text{min}$ with a flow entry angle of 45°. The resulting membranes had thicknesses in the range between 100 and 300 μm . Computational modelling of the aqueous/organic flow was performed in order to characterise flow stability and wall shear stress patterns. The flow arrangement establishes a principle for the fabrication of micromembrane structures designed for low sample volume separation, where the forming reaction is a facile and rapid interfacial process.

Keywords: Microfluidics; Nylon; Membranes; *In situ* formation; Interfacial reaction

1. Introduction

Microchip or microreaction technology has been the focus of much attention in recent years [1]. Various kinds of effective chemical processes have been successfully integrated into microchips to realise micrototal analysis (μ TAS) microreactors and lab-on-a-chip systems [2,3,4]. Controlled laminar flows in microfluidic devices have been utilised to great benefit in a number of industrial applications including diffusion-based separation and detection [5], solvent extraction [6], mixing [7] and hydrodynamic focusing [8].

In 1999, Kenis et al. [9] proposed multiphase laminar flow patterning - a method of microfabrication based on multicomponent laminar flow inside microchannels. The core idea of the method was to utilise laminar streams of aqueous solutions carrying desired reagents in order to establish a reaction at the interface between the streams. This approach not only provided the advantage of containing the reaction in a controlled thin zone but also allowed modification of the geometry of this reaction zone. The resulting reactions produced various microstructures such as continuous silver wires, used as reference electrodes, deposited polymeric structures and self-assembled monolayers.

Use of this concept and exploitation of multiphase flow using liquids of the same or similar nature, especially aqueous/aqueous, for analytical or fabrication purposes have been extensively discussed [9-11]. However, flow control of solvents with distinct properties, notably aqueous/organic, for such applications have only recently been reported. Hisamoto et al. [12-15] successfully demonstrated that highly efficient molecular transport between two phases for analytical and synthetic applications was achievable using such aqueous/organic multilayer flows; here the organic solvents used included butyl acetate and dichloroethane. Such reactions exploited the characteristics of the liquid microspace whereby short molecular diffusion distances and large specific interfacial areas could be realised. Based on these results, they advanced an approach

specifically for fabricating nylon 6,6 membranes using two immiscible laminar flows, respectively of adipoyl chloride in dichloroethane and hexamethylenediamine in aqueous solution [15]. The membranes were observed by SEM and characterised by gas permeation of ammonia. Zhao et al. [16] also reported similar nylon membrane formation inside millimetre-sized fluidic devices by using countercurrent flows of hexamethylenediamine in aqueous solution and adipoyl chloride in xylenes. The resulting nylon membranes were produced by an interfacial polycondensation reaction (Fig. 1).

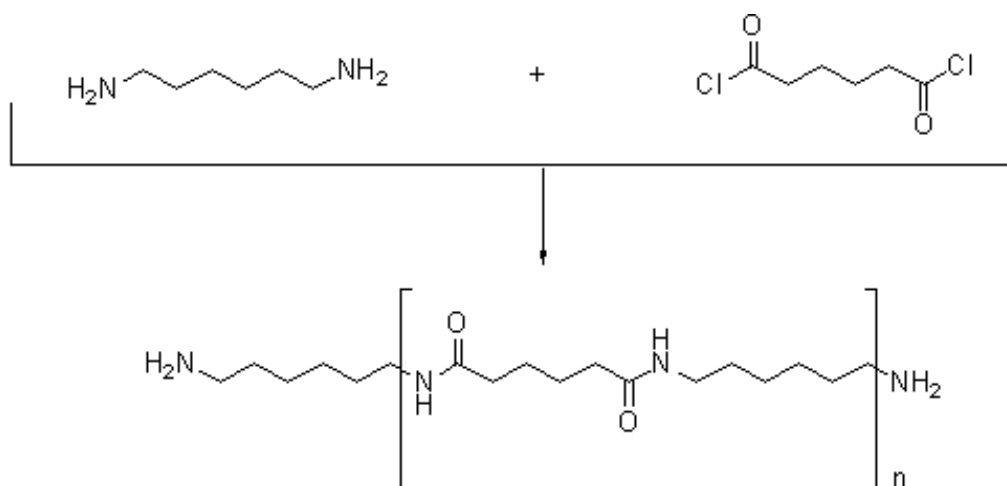


Fig. 1. The scheme of the interfacial polymerisation leading to Nylon 6,6 formation

Such interfacial polymerisation reaction is extremely fast and allows the rapid formation of tough, solid and homogeneous membranes at the aqueous/organic interface. These polymeric barriers provide controlled transport of gas molecules. Reaction rates of aliphatic acid chlorides with primary amines were reported as ranging from 10^2 up to 10^4 L.mol⁻¹.s⁻¹ in homogeneous solutions [28]. The upper value of 10^4 L.mol⁻¹.s⁻¹ was used to assess the fastest characteristic time of reaction at the interface, which was used in the timescale analysis in Section 3.1 of this paper. The kinetics and mechanisms of polycondensation in a two-phase system depends in part on the nature of the solvents. One of the solvents is usually water as it dissolves both the diamine and the low molecular weight reaction product (ammonium salts). The choice of organic solvent is important however because it dominates the distribution of reagents between the two phases, diffusion behaviour of the reagents as well as polymer swelling and permeability [31].

Conventional methods for membrane fabrication usually rely on either wet or immersion casting, polymerisation, phase inversion on solid substrates by solvent evaporation, spin-coating or electropolymerisation. Membranes formed in this manner can be quite thick, or may need a backing support, and their permeability properties are difficult to control. However, for spin-coating, there is a similarity with the present system in that interfacial shear varies with spin speed, which does impact membrane thickness.

Suspended membranes proposed here, and formed as an initial phase separation layer at a controlled laminar flow interface could provide a route to barrier film formation with the potential to allow for new solute permeability profiles using existing materials. Such a separation of chemical species, based on both chemical and physical outcomes of the forming process, could be further modified by the addition of chemical inclusions (e.g. lipids, surfactants, enzymes) or by surface modification. Resulting suspended walls inside microchannels could be used in microseparation, microreactions as well as biochemical analysis. Controlled *in situ* formation/degradation of such membranes could also lead the way to the use of “intelligent” valves, with an ability to redirect flows to specific channels [17].

The study presented in [15] serves as a “proof-of-concept” for the laminar flow patterning method of polymer membrane fabrication (see Fig. 2). However, little is known about the influence of the microfluidic device geometry and carrier liquid flow rates on the formation of polymer membranes at the interface.

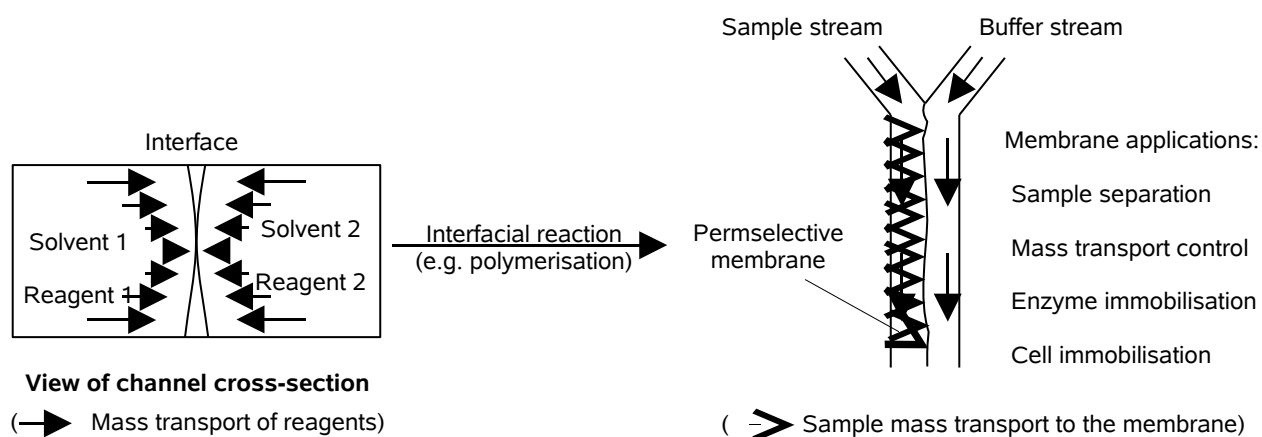


Fig. 2. Schematic of polymer membrane formation at the interface between two solvents.

Apart from the reaction kinetics, the initial stages of membrane formation are influenced by two physical phenomena - the flow of the carrier liquids and the diffusion of the reagents. The first phenomenon - diffusion between two laminar streams in a microchannel has been studied by a number of researchers analytically [18,19], experimentally [5,19,20] and numerically [18,20] and the effects of reagent delivery on the initial stages of a diffusion governed reaction is fairly well understood. However the second issue, the stability of the carrier liquid flow, proves to be more difficult to analyse. Although low Reynolds numbers (<100) of the microflows typically used in microfabrication applications ensure that flow occurs free from shear-induced instabilities [21], the jump of viscosity and density across the carrier liquids can induce interfacial instabilities even at very low Reynolds numbers [22,23,24]. Most of the studies of this interfacial instability available in the literature are focused on two-dimensional flows and the stability of the interface between streams of different liquids for essentially three-dimensional microfluidic geometries is difficult to analyse theoretically.

In this study we consider experimentally the formation of nylon 6,6 membrane using the same reaction as in [15] with xylene and high-purity deionised water used as carrier liquids for adipoyl chloride and hexamethylenediamine respectively, in order to analyse the influence of microfluidic device geometry and flow rates on the membrane formation. We also perform numerical simulation of the carrier liquids flow using both commercially available CFD package (FLUENT) and in-house codes developed for variable density multicomponent flows [25,26], in order to estimate the stability of the experimental flow configuration and analyse the near-wall shear stresses affecting membrane attachment.

2. Experimental

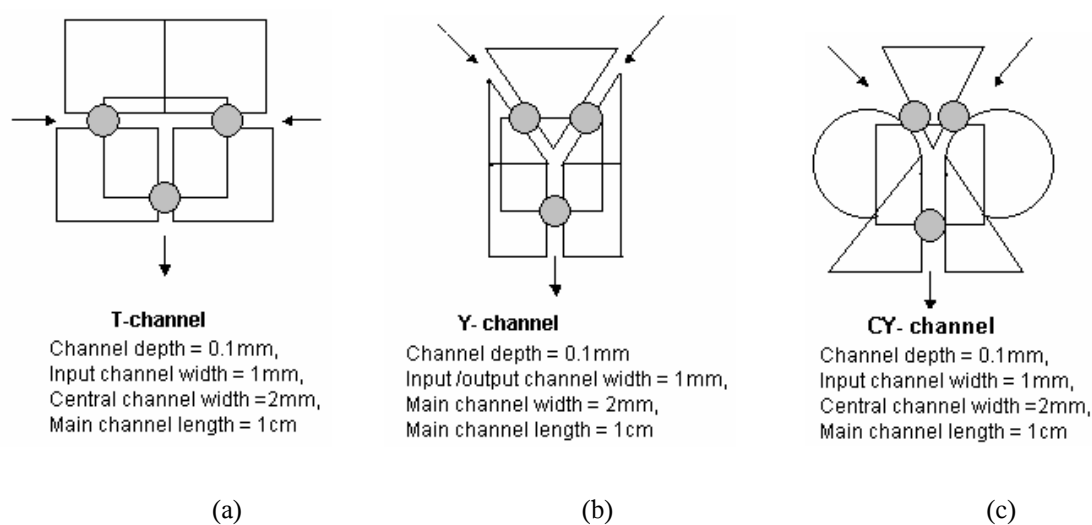
2.1. Chemicals

Reagents of the highest grade commercially available were used for the preparation of the

aqueous and organic phases and synthesis of nylon 6,6 by interfacial polycondensation. Adipoyl Chloride, hexamethylenediamine and xylene were purchased from Aldrich. High-purity deionised water was used for preparation of the aqueous phase.

2.2. Flow structure fabrication

The structures tested for controlled flow entry were based on various geometries. Each of these was fabricated in house using microscope glass slides (52 mm x 76 mm, thickness of 1.2mm) as the lower base and cover slips (22 mm x 22mm, thickness of 0.1 mm) as channel sidewalls. These walls were obtained by cutting the glass cover slips and bonding them in the correct geometrical arrangement onto the lower glass plate using a UV-curable adhesive, Loctite 3211, purchased from Loctite (UK). The top of the channel was sealed using a full uncut cover slip (22 mm x 22mm) bonded to rest of the structure in a similar manner. By this method, a wide variety of flow structures were assembled (Fig. 3). Input and output connectors were fabricated by UV-bonding the conical tips (5 mm) of conventional Eppendorf pipettes (Type D, blue, 50-1000 μ l capacity, purchased from VWR, UK) to entry and exit channels of the flow structures. Finally, in order to ensure proper sealing of channels and to prevent leakage, all junctions were sealed using an additional layer of epoxy resin (Araldite®) and left to set overnight.



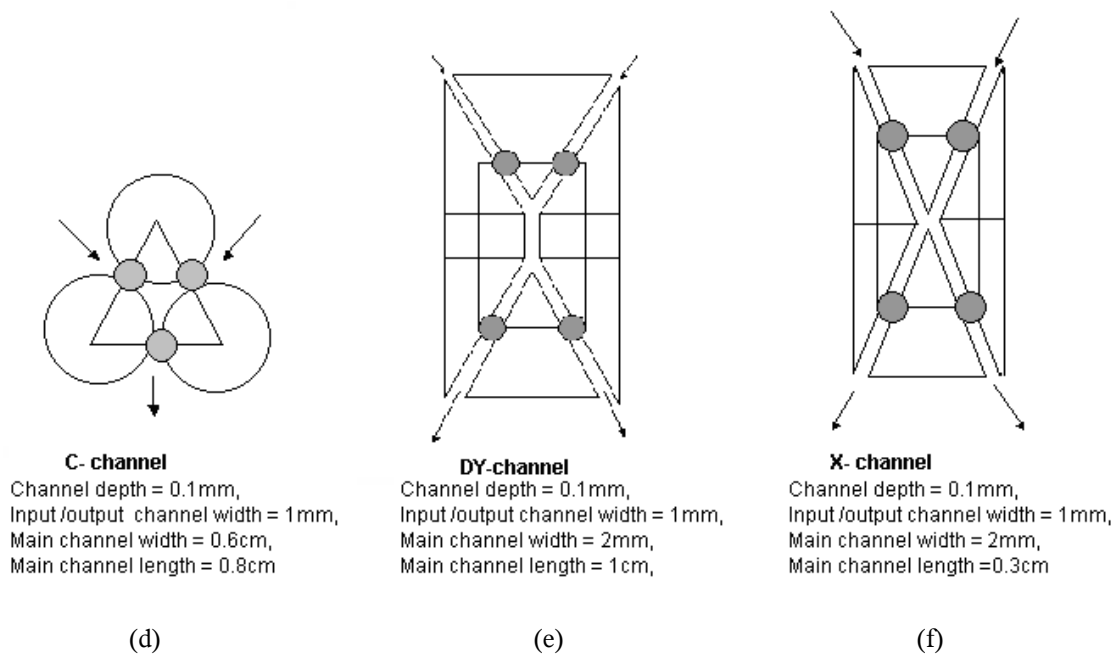


Fig. 3. Schematics of the various flow structures used for this study. (Shaded circular areas are points of fluid entry and locations of pipette tips)

2.3. Flow protocols

Pressure driven flow was generated using a KdScientific 200 syringe pump, purchased from Royem Scientific Ltd (UK), fitted with two 10ml glass syringes (14.67 mm inner diameter), allowing for flow rates range between 0.001 $\mu\text{l/h}$ and 20.91 ml/min. For each experiment, single nylon structures were prepared inside the various flow structures. For that purpose, adipoyl chloride in xylene (62.5 mM) and hexamethylenediamine in 0.1 M NaOH solution (62.5 mM) were prepared and used as organic and aqueous immiscible phases. For each experiment, both solutions were injected simultaneously with identical flow rates. Various volume flow rates (500, 1000, 2000 and 4000 $\mu\text{l/min}$, respectively) were used for preparing the single nylon membrane structures. Images were captured by a Motic BA400 trinocular microscope (purchased from VWR), fitted with a Moticam 1000 high-resolution (1280x1024) digital camera.

3. Results and discussion

3.1. Carrier flow analysis

Adipoyl chloride and hexamethylenediamine are supplied into the main channel where the reaction takes place, as dilute solutions of the carrier liquids, i.e., xylene and deionised water, respectively. The effect of the solute on the bulk density and viscosity of these solutions is negligible.

Flow development in the channel depends on the timescale associated with pressure waves propagation through water; the estimate for the flow development time, based on the speed of sound in water [27] and half channel width, yields a value of approximately 7×10^{-7} s. The time required for completion of Nylon 6,6 formation, based on a rate constant of 10^4 L.mol⁻¹.s⁻¹ [28] and reagent concentration, is approximately 2×10^{-3} s. Using the estimates of diffusion coefficient according to empirical molecular weight correlation [29,30], it is possible to determine the diffusion time as being of the order of 10^3 s for half channel width transfer. Finally, the time of convection, based on the average velocity and channel half-width, varies from 1.2×10^{-2} s to 1.5×10^{-3} s for the range of flow rates used (500 – 4000 μ L/min.). From these estimates, it is possible to conclude that the timescale of the polymerisation process is much greater than the timescale of flow development. Therefore, at the initial stages of membrane formation, the hydrodynamics of the problem is dominated by the developed flow of the carrier liquids.

The computational aspect of this study was motivated by the need to shed light on the effects of shear stresses induced by the carrier-liquid flows, which could possibly prevent the attachment of formed nylon to the walls of the microfluidic channel. When nylon forms at the interface, the viscosity is locally increased, thereby increasing shear stress. Therefore, shear-stress values of the carrier liquids provide the lower-bound for the shear stress at the initial stages of membrane formation. Furthermore, although the Reynolds numbers occurring in this case are fairly small, ranging from $Re = 8.4$ to 67.2 , based on water properties and channel depth, the flow of two fluids in a channel can develop interfacial instabilities even at low Reynolds numbers [22,23,24].

The flow was modelled as a variable-density multispecies flow of immiscible fluids, for which a

set of Navier-Stokes equations was solved together with an advection equation for the density of xylene [25,26].

In order to investigate the flow of carrier liquids, we also carried out a computational investigation of a Y-inlet channel with a 45 degrees inlet angle, for the maximum and minimum values of the flow rates considered in the experiment. The results of these simulations are summarised below.

Since gravity force acts on the plane of the interface between the carrier fluids, both flow stability and the developed flow velocity profile depend primarily on the ratio of viscosities of the carrier liquids. The dynamic viscosity of xylene depends on the isomer composition and so varies between 0.62 and 0.76 mPa. In order to estimate the influence of viscosities ratio, computations for the maximum and minimum possible viscosity of xylene were carried out.

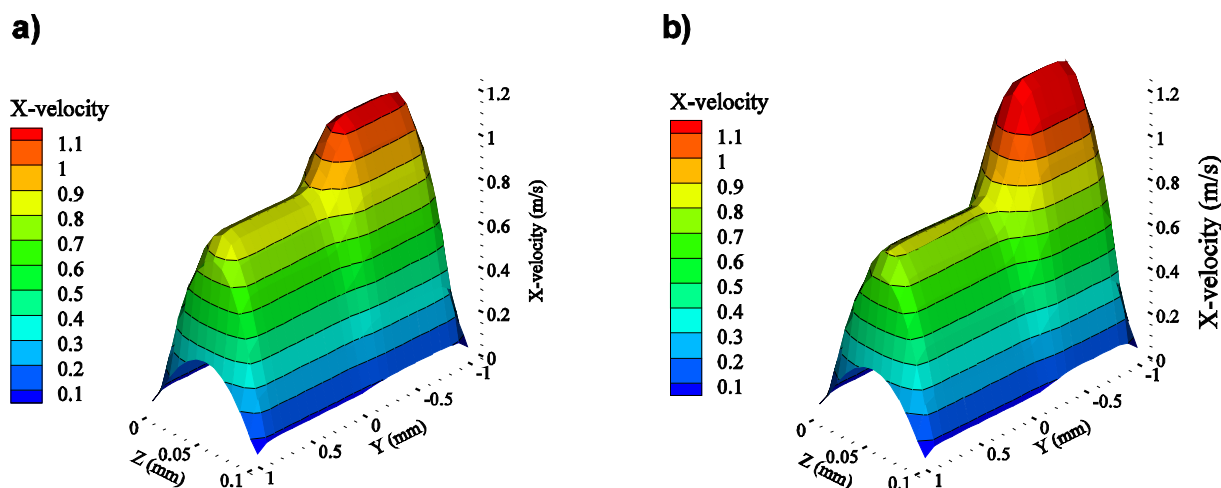


Fig. 4. Developed velocity profiles for maximum (a) and minimum (b) xylene viscosity.

Depending on the flow rate, the length required for the flow to become fully developed in the main channel varies from 2 to 6 channel widths (entrance length). Once the flow has been fully developed the dominant component of the velocity is the streamwise (or X in our co-ordinate system). From the velocity profiles it can be seen that the interface between xylene and water tends to shift towards xylene. Fig. 4 shows an example of the developed velocity profile in the cross-section of the main channel at a flow rate of 4000 $\mu\text{l}/\text{min}$ for maximum (Fig. 4a) and minimum (Fig.

4b) dynamic viscosities of xylene. In this figure, the region with lower velocity corresponds to the carrier liquid with lower viscosity (xylene). The flow was found to be stable for both values of dynamic viscosity. The interface between xylene and water tends to shift towards xylene. This effect is explained by the fact that the same flow rates are maintained in both inlets. Thus, in order to achieve a given flow rate, the carrier liquid moving at a higher velocity needs a smaller cross-section. The displacement of the interface increases when increasing the flow rate and water/xylene viscosity ratio (Fig. 5).

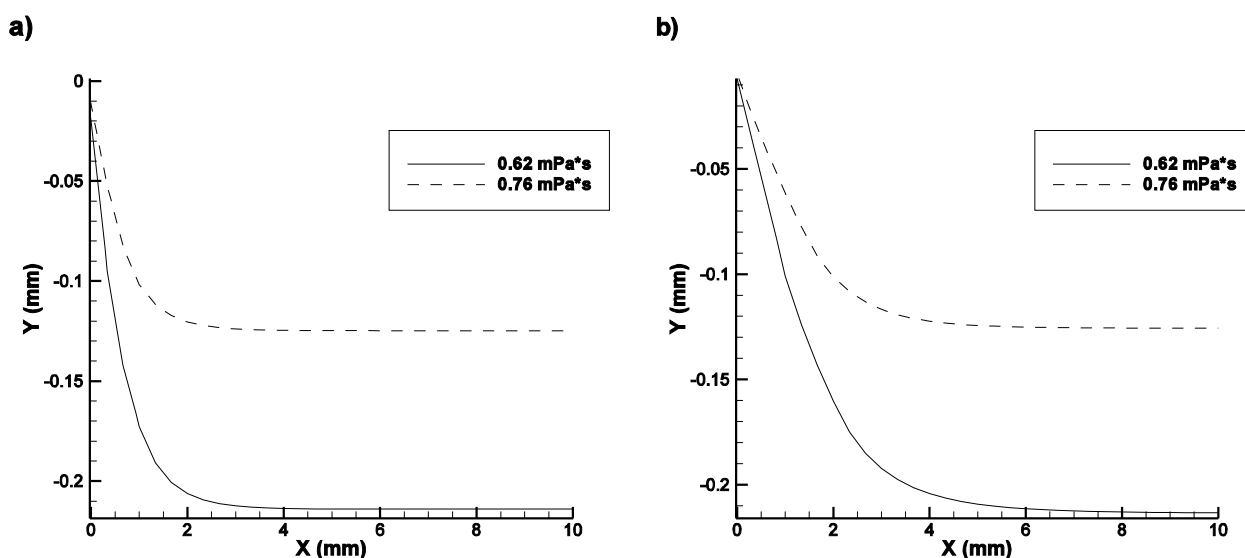


Fig. 5. Interface position in the middle of the channel: a) $Q=500 \mu\text{l}/\text{min}$; b) $Q=4000 \mu\text{l}/\text{min}$.

Fig. 6 shows the values of the shear stress at the upper wall of the microfluidic channel for different flow rates/viscosities of xylene plotted on the line of the interface between the liquids. Wall shear stress increases linearly with flow rate, so shear stress can reach large values preventing membrane attachment to the wall. On the other hand, shear stress is seen to drop near the entrance of the microfluidic channel, where the initial membrane formation takes place.

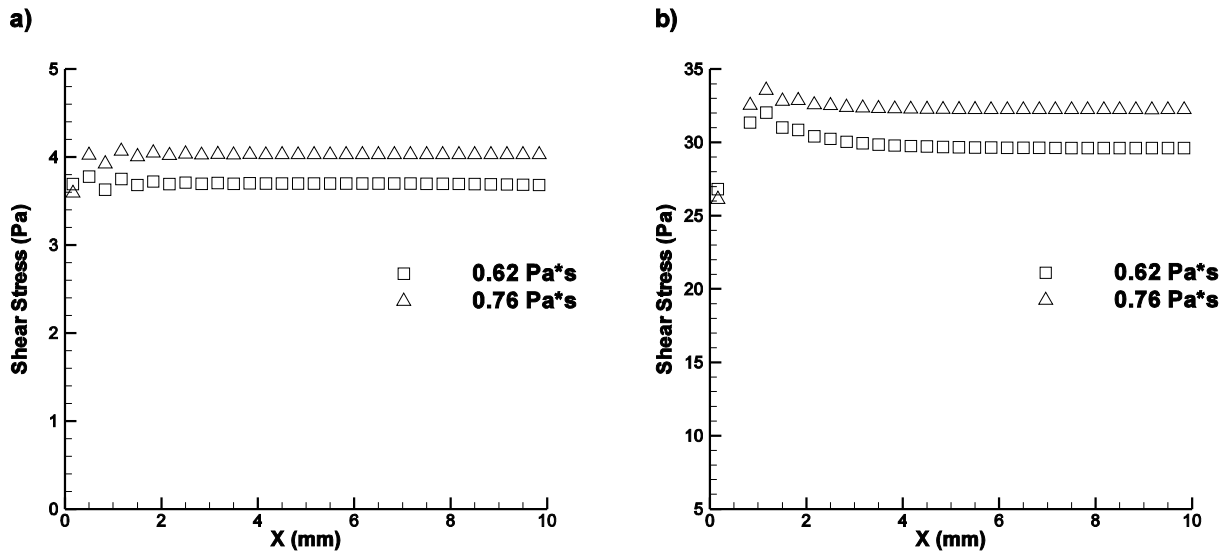


Fig. 6. Wall shear stress along the interface between the carrier liquids:

a) $Q=500 \mu\text{l}/\text{min}$; b) $Q=4000 \mu\text{l}/\text{min}$.

Computations were also performed for a T-inlet channel revealing similar trends to the Y-channel case for the effect of xylene viscosity and flow rates. However, the T-geometry favours a lower velocity at the interface between the two liquids at the beginning of the channel. Fig. 7 shows the magnitude of the velocity at the interface between xylene and water in the middle of the channel as a function of the channel length.

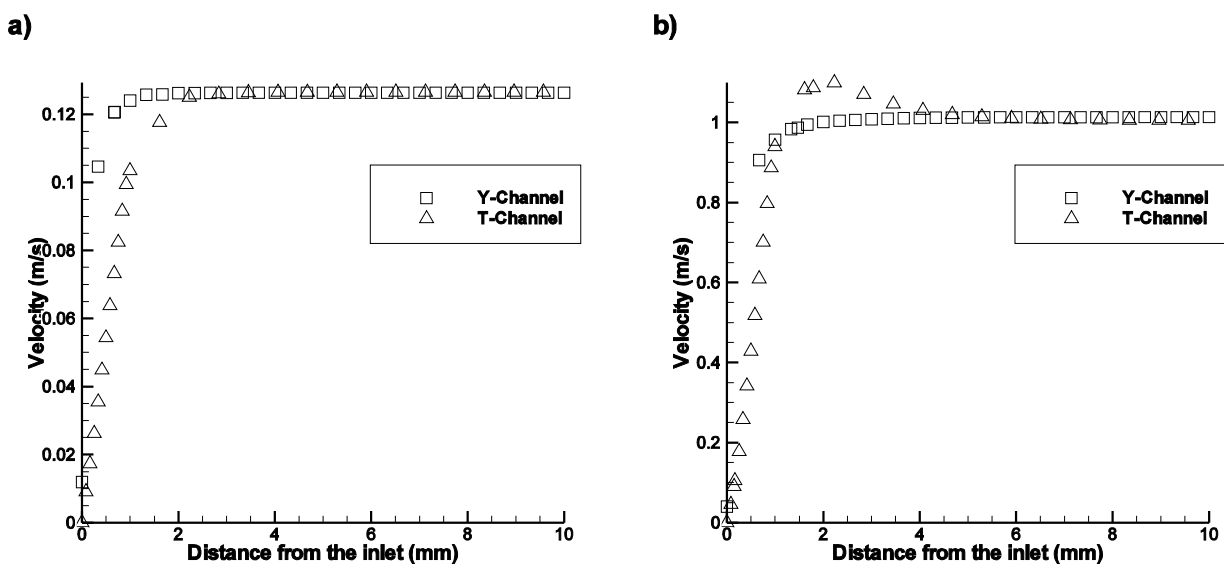


Fig. 7. Velocity magnitude along the interface between the carrier liquids in the middle of the

channel: a) $Q=500 \mu\text{l}/\text{min}$ b) $Q=4000 \mu\text{l}/\text{min}$.

T-channel geometry exhibits non-uniform velocity profile development at high flow rates, which may lead to non-uniform membrane formation.

3.2. Membrane formation

Polycondensation of Nylon 6,6 is a rapid reaction at the solution interface and was achieved using various flow structures, including a Y-shaped flow device (Fig.8) which was favoured by the simulation studies with respect to membrane stability and quality.

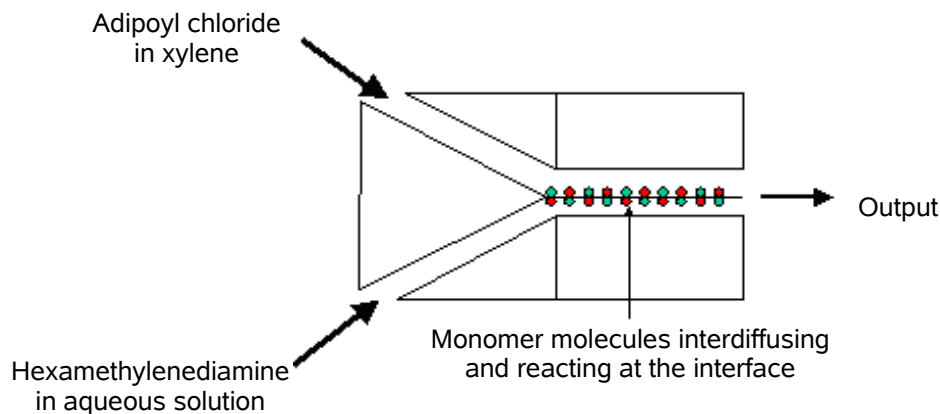


Fig. 8. Schematic of a Y- channel for dual organic/aqueous solution entry and membrane formation.

A key requirement for the interfacial condensation here is the stable liquid-liquid interface. Under the current arrangements, a stable interface between dual laminar flows of xylene and water was observed at all flow rates (Fig. 9) in accordance with the numerical results. Minor interface deviation at 4000 $\mu\text{l}/\text{min}$ is thought to be due to the imperfection of the channel entrance. The deviation of the interface towards the side of the less viscous fluid (xylene) is more visible for low flow rates. 2000 $\mu\text{l}/\text{min}$ appeared to be ideal for optimum stability and was used for *in situ* fabrication and to help provide a continuous membrane at the interface between xylene and water in laminar flows.

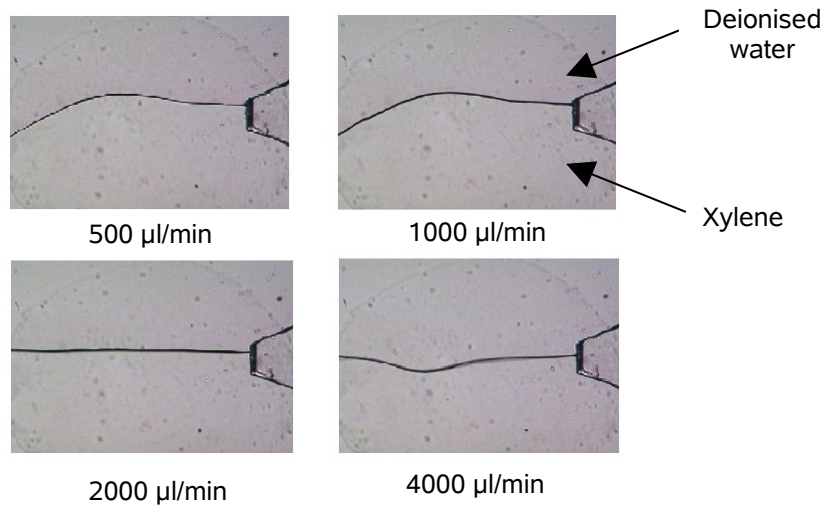


Fig. 9. Stable laminar flow interfaces between xylene and water at various flow rates in the Y-structure (Fig. 3b).

A series of experiments was performed using the different flow cell structures. Results were critically dependent on different flow geometries and flow rates. The following represents the interaction of these two parameters on the final formed nylon membranes.

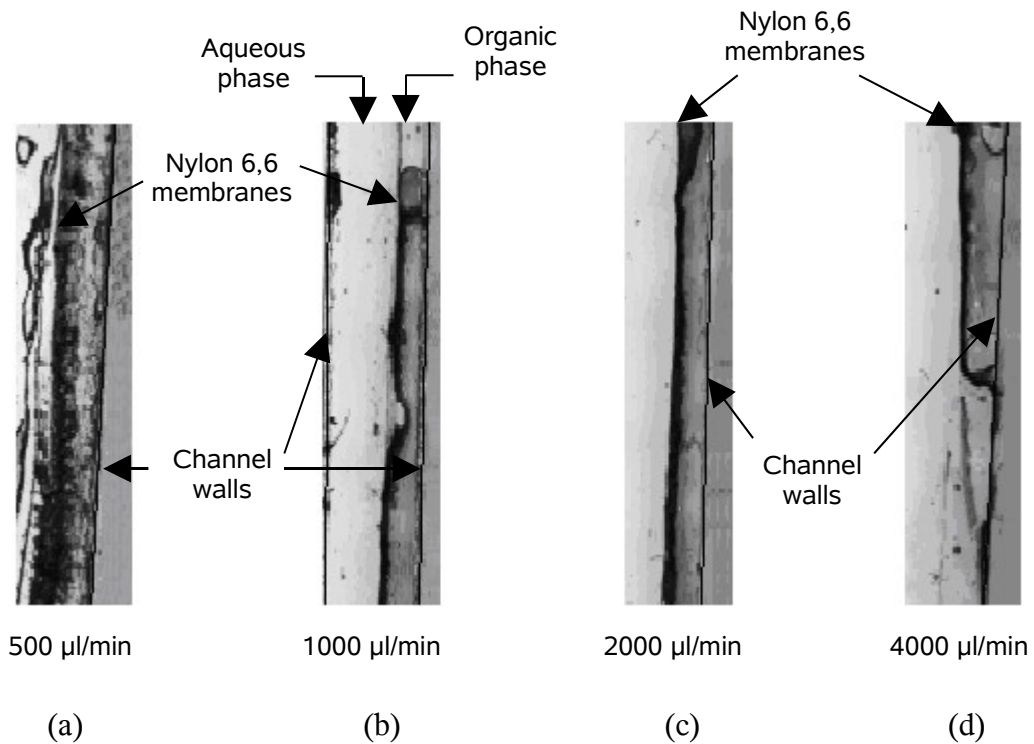


Fig. 10. Images of wet membranes obtained using T-channels at different flow rates.

For the T-channel (Fig. 3a), dual liquid flow rates were varied in line with those in Fig. 9. Membrane structures that formed in each case were incomplete along the 1cm channel length. Consistent with the observations made using liquid-only flows (Fig. 9), the most even and continuous membrane structures were seen at 2000 $\mu\text{l}/\text{min}$. Above and below this flow rate, there was considerably greater unevenness and failure of complete membrane formation (Fig. 10). Thus, for 500 $\mu\text{l}/\text{min}$ (Fig. 10a), coarse and uneven structures of approximately 300 - 500 μm thicknesses were deposited. This would suggest that, despite diffusion limitation and a thicker unstirred Nernst layer compared with rapid flow, more polymer formed at the interface. A possible explanation for this is the greater shear forces at higher flow rates leading to the removal of nascent polymer material, thus leaving only the consolidated central film. This seems to be confirmed by the fact that, at higher flow rates (Fig. 10b-c), thinner (100 μm thickness) and more even membranes were produced. Furthermore, the disruption of the membrane observed at 4000 $\mu\text{L}/\text{min}$. (Fig. 10d) could be the result of extremely high shear forces acting on an already thin, hence more fragile membrane.

These results indicate the fragility of the initial formed structures, problems of surface adhesion and the high impact of minor flow asymmetry. Importantly, therefore, varying flow rate had a marked influence on the quality of formed membranes. In all cases, the Reynolds numbers were low (less than 70). Equivalent studies were made using the other flow cell structures, shown in Fig. 3.

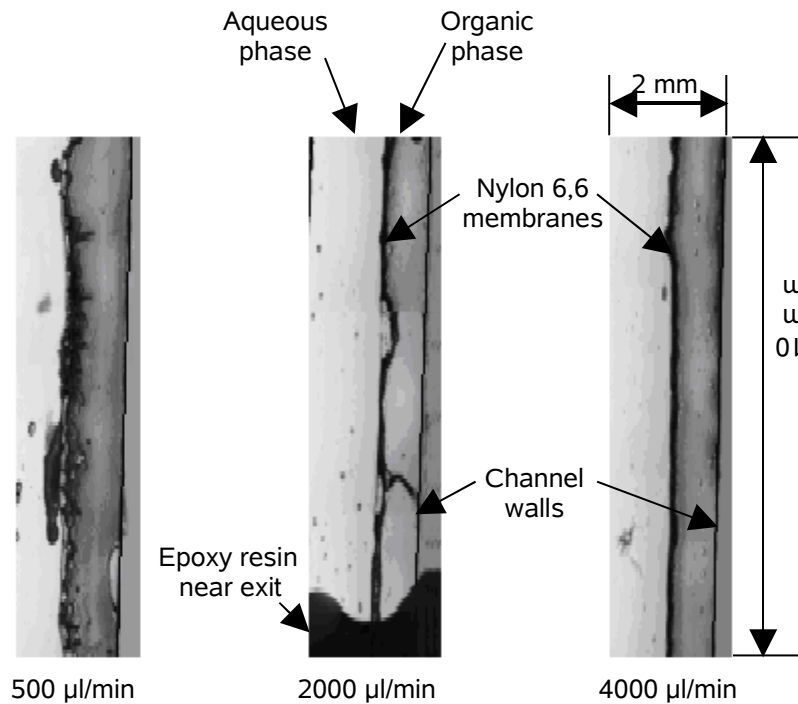


Fig. 11. Images of membranes obtained using Y-channels at different flow rates.

For the membranes obtained using Y-channels (Fig. 3b), performance improved giving better quality membranes at high flow rates (Fig.11), with the same trend towards more even, continuous and thinner structures as flow rate increased. The significant improvement over the quality of generated membranes compared with T-channels is apparently due to the orthogonal line of approach of the fluids in these structures, which as computations indicate, should result in thicker membrane in the inlet, which is indeed observed in the experiment. Higher flow rates lead to the reduction of the reaction zone, however the velocity profile development then becomes non-uniform (see Fig. 11).

The Y-shaped structure, with an input angle of 45° , offers a smoother development of the velocity profile at the fluid interface, which results in thinner membrane near the inlet. Again, as the flow rate increases, the reaction zone becomes even thinner, which facilitates the development of a smooth membrane.

The CY-channel (Fig. 3c) features a curved entry point near the walls. This was intended to reduce any initial perturbations.

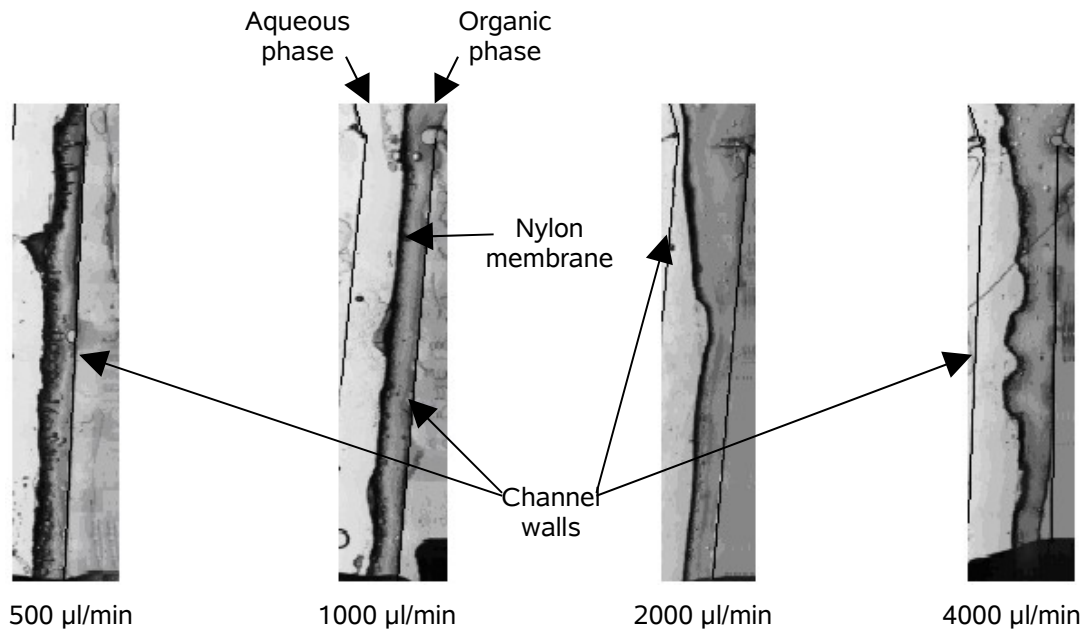


Fig. 12. Images of membranes obtained using CY-channels at different flow rates.

With the CY-channel, the quality of the resulting membranes improved over that obtained using both T- and Y-shaped flow structures. For all flow rates, membranes were firmly anchored. They appeared to be continuous and showed no breaks (Fig. 12). This overall improvement can be explained by the smooth parabolic entry of fluids into the main channel, orienting the fluids in a longitudinal direction parallel to the channel walls, thus preventing the build-up of an overpressure and, consequently, helping the membrane to form, attach and grow more uniformly along the length of the flow structure.

Again, for the CY-channel, membranes resulting from fluids injected at low flow rates were substantially thicker than those obtained with fluids at high flow rates. This underlines the importance of residence time in controlling lateral transport of precursors to the interface. Because of the advantage seen with entry curvature, a specific structure, the C-channel (Fig. 3d) was investigated, which had curvature at the main channel.

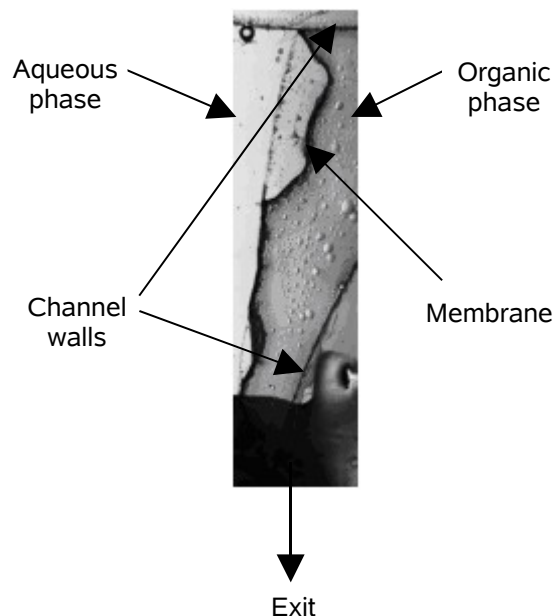


Fig. 13. Image of membrane obtained using C-channel at 4000 $\mu\text{l}/\text{min}$.

This structure however failed to generate stable solvent interfaces, and uneven, fragmented and laterally displaced membranes were produced regardless of flow rate (channel width here changed from entry: 2 mm to exit: 0.6 mm), and due to this, a gradient of velocities was likely to have been created towards the channel exit. This will have affected flow symmetry despite a nominal symmetry to this flow cell. However, the entry angle for the fluids was 120° , making this structure closer to a T-channel than a Y-channel design, which would also promote the build-up of an overpressure near the entry point, typical of high entry angles. This geometry is currently unsuitable but the integrity of membrane structures at high flow rates (Fig. 13) suggests that, with further optimisation, there may be a possibility to harness convergent compressive forces to stabilise formed layers.

All the above flow structures featured a single output channel without a second exit anchoring point where the membrane could more easily attach to be better held inside the fluidic assembly. Therefore, a symmetrical double Y shape (DY-channel) was designed (see Fig. 3e) and used to study the impact of a dual angular outflow. Here, both inputs and outputs were at an angle of 45° .

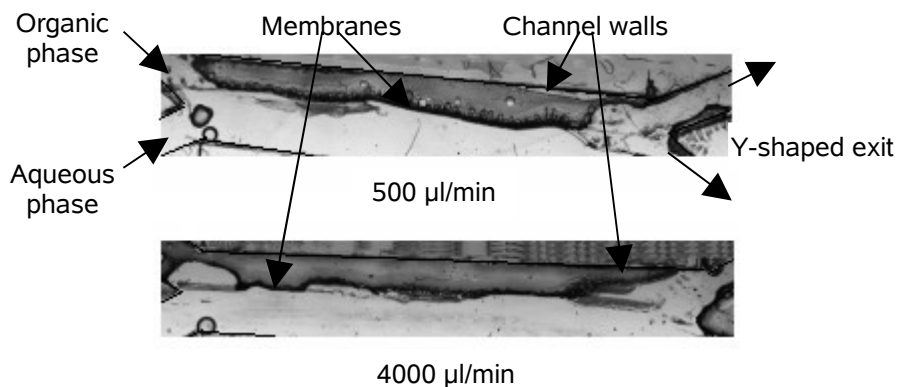


Fig. 14. Images of membranes obtained using DY-channels at different flow rates.

The outcome, however, was high flow asymmetry, with selective lateralisation of outflows and shifting of formed membranes to one or other wall (Fig. 14). The preferential nylon deposition towards one outlet then led to build-up of backpressure on that side and asymmetry at the entire membrane. With the X-channel construct (Fig. 3f), no discrete membrane formation was possible. Despite the proximity of two attachment points and clear flow symmetry, no stable laminar dual phase could be established.

4. Conclusions

Various flow structures and flow conditions were used to demonstrate the major impact that both channel geometry and flow rate have on the quality of generated nylon 6,6 membranes generated *in situ* by interfacial polycondensation. The best membranes were observed for Y-shaped structures with a 45° entry angle, curved input walls and a single exit. This was favoured both by laboratory experiments and computer simulations performed in the course of this study. The combination of these geometrical features and a flow rate of 2000 µl/min reduced the likelihood of overpressure at the entry of the channel. This allowed the nylon 6,6 membranes to attach and to grow so as to generate a linear, continuous, thin and even membrane from the Y-junction down to the exit of the channel. This membrane is parallel to the walls of the channels thanks to the lateral shear forces exerted by the two immiscible laminar fluids onto the film.

The analysis of shear stresses indicates that the near-wall stresses increase linearly with the flow rate and can reach large values preventing membrane attachment to the wall. This effect can be responsible for non-uniform membrane formation at high flow rates. Note that the flows at the Reynolds numbers and viscosity ratios considered here remain laminar irrespective of the flow cell design. Therefore, the differences observed are not associated with turbulent flow effects but are due to the effects of the geometry on the flow development particularly near the entrance region.

Future work will emphasize smaller entry angles and the further testing of the attachment profiles of membranes to the channel structures. It is likely that this basic system can be extended to the use of copolymers, blends, lipids and surfactants to modulate bulk and surface properties for transport control.

Acknowledgment

The investigation was performed with the financial support of the Engineering and Physical Sciences Research Council (GR/S13668).

References

- [1] M. Freemantle, Microscale technology, Chem. Eng. News, February 22 (1999), 27-36
- [2] J.M. Ramsey and A. van den Berg, Proceedings of the μ TAS'2001 Symposium 2001, Kluwer Academic Publishers: Dordrecht, The Netherlands (2001)
- [3] W. Ehrfeld, Proceedings of the Third International Conference on Microreaction Technology, Springer: Berlin (1999)
- [4] W. Ehrfeld, V. Hessel and H. Lowe, Microreactors: New Technology for Modern Chemistry, Wiley-VHC: Weinheim (2000)
- [5] B.H. Weigl and P. Yager, Microfluidic diffusion-based separation and detection, Science, 283 (1999) 346-347

- [6] W.E. TeGrotenhuis, R.J. Cameron, M.G. Butcher, P.M. Martin, R.S. Wegeng, Microchannel devices for efficient contacting of liquids in solvent extraction, *Separation Science and Technology*, 34 (1998) 951-974
- [7] P.K. Wong, Y.K. Lee and C.M. Ho, Deformation of DNA molecules by hydrodynamic focusing, *J. Fluid. Mech.*, 497 (2003) 55-65
- [8] N.T. Nguyen and Z. Wu, Micromixers – a review, *J. Micromech. Microeng.*, 15 (2005) R1-R16
- [9] P.J.A. Kenis, R.F. Ismagilov and G.M. Whitesides, Microfabrication inside capillaries using multiphase laminar flow patterning, *Science*, 285 (1999) 83-85
- [10] A.E. Kamholtz, B.H. Weigl, B.A. Finlayson and P. Yager, Quantitative analysis of molecular interaction in a microfluidic channel: the T-sensor, *Anal. Chem.*, 71 (1999) 5340-5347
- [11] P.J.A. Kenis, R.F. Ismagilov, S. Takayama, G.M. Whitesides, S. Li and H.S. White, Fabrication inside microchannels using fluid flow, *Acc. Chem. Res.*, 33 (2000) 841-847
- [12] H. Hisamoto, T. Horiuchi, M. Tokeshi, A. Hibara and T. Kitamori, On-chip integration of neutral ionophore-based ion pair extraction reaction, *Anal. Chem.*, 73 (2001) 1382-1386
- [13] H. Hisamoto, T. Horiuchi, K. Uchiyama, M. Tokeshi, A. Hibara and T. Kitamori, On-chip integration of sequential ion-sensing system based on intermittent reagent pumping and formation of two-layer flow, *Anal. Chem.*, 73 (2001) 5551-5556
- [14] H. Hisamoto, T. Saito, M. Tokeshi, A. Hibara and T. Kitamori, Fast and high conversion phase-transfer synthesis exploiting the liquid-liquid interface formed in a microchannel chip, *Chem. Commun.*, (2001) 2662-2663
- [15] H. Hisamoto, Y. Shimizu, K. Uchiyama, M. Tokeshi, Y. Kikutani, A. Hibara and T. Kitamori, Chemicofunctional membrane for integrated chemical processes on a microchip, *Anal. Chem.*, 75 (2003) 350-354
- [16] B. Zhao, N.O.L. Viernes, J.S. Moore and D.J. Beebe, Control and applications of immiscible liquids in microchannels, *J. Am. Chem. Soc.*, 124 (2002) 5284-5285

- [17] J. Atencia, D.J. Beebe, Controlled microfluidic interfaces, *Nature*, 437 (2005) 648-655
- [18] A.E. Kamholtz and P. Yager, Theoretical analysis of molecular diffusion in pressure-driven laminar flow in microfluidic channels, *Biophysical Journal*, 80 (2001) 155-160
- [19] R.F. Ismagilov, A.D. Stroock, P.J.A. Kenis and G.M. Whitesides, Experimental and theoretical scaling laws for transverse diffusive broadening in two-phase laminar flows in microchannels, *Appl. Phys. Lett.*, 76 (2000) 2376-2378
- [20] K.B. Greiner, M. Deshpande, J.R. Gilbert, R.F. Ismagilov, A.D. Stroock and G.M. Whitesides, Design, analysis and 3D measurement of diffusive broadening in a Y-mixer, *Technical Proceedings of Micro Total Analysis Systems, Enschede, The Netherlands, MicroTAS (2000)* 87-90
- [21] P.G. Dreizin, W.H. Reid, *Hydrodynamic Stability*, Cambridge University Press (2004)
- [22] C.S. Yih, Instability due to viscosity stratification, *J. Fluid. Mech.*, 27 (1967) 337-352
- [23] S. G. Yiantsios, B. G. Higgins, Linear stability of plane Poiseuille flow of two superposed fluids, *Phys. Fluids*, 31 (1988) 3225-3238
- [24] D. D. Joseph, Y. Y. Renardy, *Fundamentals of Two Fluid Dynamics: Mathematical Theory and Applications*, Pt. 1 (Interdisciplinary Applied Mathematics), Springer-Verlag Berlin and Heidelberg (1993)
- [25] E. Shapiro and D. Drikakis, Artificial compressibility, characteristics-based schemes for variable density, incompressible, multi-species flows. Part I. Derivation of different formulations and constant density limit, *J. Comp. Phys.*, 210 (2005) 584-607
- [26] E. Shapiro and D. Drikakis, Artificial compressibility, characteristics-based schemes for variable-density, incompressible, multispecies flows: Part II. Multigrid implementation and numerical tests, *J. Comp. Phys.*, 210 (2005) 608-631
- [27] J.D. Cutnell and K.W. Johnson, *Physics*, New York: Wiley (1997), 468.
- [28] P.W. Morgan and S.L. Kwolek, Interfacial polycondensation. II. Fundamentals of polymer formation at liquid interfaces, *Journal of Polymer Science*, XL (1959), 299

- [29] J. Georges, Investigation of the diffusion coefficient of polymers and micelles in aqueous solutions using the Soret effecting cw-laser thermal lens spectrometry, *Spectrochimica Acta Part A*, 59 (2003), 519
- [30] V. Murugaiah, R.E. Synovec, *Anal. Chim. Acta*, 246 (1991), 241
- [31] V.V. Korshack and V.A. Vasnev, *Comprehensive Polymer Science*, Volume 5, chapter 11 (1990), 167